

Delayed-enhancement magnetic resonance simulation imaging for prone radiotherapy after breast-conserving surgery: Assessing its application in lumpectomy cavity delineation based on deformable image registration

changhui Zhao (✉ 1732329000@qq.com)

Shandong University School of Medicine: Shandong University Cheeloo College of Medicine

Jianbin Li

Shandong Cancer Hospital: Shandong Cancer Hospital and Institute

Wei Wang

Shandong Cancer Hospital: Shandong Cancer Hospital and Institute

Guanzhong Gong

Shandong Cancer Hospital: Shandong Cancer Hospital and Institute

Liang Xu

Shandong Cancer Hospital: Shandong Cancer Hospital and Institute

Yingjie Zhang

Shandong Cancer Hospital: Shandong Cancer Hospital and Institute

Fengxiang Li

Shandong Cancer Hospital: Shandong Cancer Hospital and Institute

Qian Shao

Shandong Cancer Hospital: Shandong Cancer Hospital and Institute

Jinzhi Wang

Shandong Cancer Hospital: Shandong Cancer Hospital and Institute

Xijun Liu

Shandong Cancer Hospital: Shandong Cancer Hospital and Institute

Min Xu

Shandong Cancer Hospital: Shandong Cancer Hospital and Institute

Research Article

Keywords: Prone radiotherapy, Breast-conserving surgery, Lumpectomy cavity delineation, Computed tomography simulation image, Delayed-enhancement magnetic resonance simulation image

Posted Date: March 19th, 2021

DOI: <https://doi.org/10.21203/rs.3.rs-306339/v1>

License:  This work is licensed under a Creative Commons Attribution 4.0 International License.

[Read Full License](#)

Abstract

Background

The application of delayed-enhancement magnetic resonance (DE-MR) simulation imaging in lumpectomy cavity (LC) delineation for prone radiotherapy in patients with an invisible seroma or a low seroma clarity score (SCS) after breast-conserving surgery (BCS) based on deformable image registration (DIR) was assessed.

Methods

Twenty-six patients who were suitable for radiotherapy in prone positions after BCS were enrolled, and both computed tomography (CT) and DE-MR simulation scans were acquired. The LC delineated based on titanium surgical clips on CT images was denoted as LC_{CT} . The LC delineated based on the signal of cavity boundaries on fat-suppressed T2-weighted imaging (T2WI) and multiphase delayed-enhancement T1-weighted imaging (DE-T1WI), which was performed at 2 min, 5 min and 10 min postinjection, were denoted as LC_{T2} , LC_{2T1} , LC_{5T1} and LC_{10T1} , respectively. Afterwards, DIR was performed to compare the volumes and locations of the LCs with MIM software. The generalized conformity index (CIgen) of inter (intra) observer (Inter-CIgen and Intra-CIgen) was also used to explore the inter(intra) observer variation for LC delineation on each image modality.

Results

LC_{CT} - LC_{10T1} provided the best conformal index (CI) and degree of inclusion (DI), increasing by 2.08% and 4.48% compared to LC_{CT} - LC_{T2} , 11.36% and 2.94% for LC_{CT} - LC_{2T1} , and 8.89% and 7.69% for LC_{5T1} - LC_{CT} , respectively. The center of mass (COM) of LC_{CT} - LC_{10T1} decreased by 17.86%, 6.12% and 13.21% compared with that of LC_{CT} - LC_{T2} , LC_{CT} - LC_{2T1} and LC_{CT} - LC_{5T1} , respectively. The agreement of LC delineation was strongest for 10th min DE-T1WI (coefficient of variation, COV = 2.30%, Inter-CIgen = 87.06%, Intra-CIgen = 92.64%).

Conclusion

For patients with a low SCS ($SCS \leq 2$) after BCS, it is feasible to contour the LC based on prone DE-MR simulation images. Furthermore, the LC derived from prone DE-T1WI at 10 min was found to be most similar to that derived from prone CT simulation scans using titanium surgical clips regardless of the volume and location of the LC. Inter(intra)variability was minimal for the delineation of the LC based on 10th min DE-T1WI.

Background

Breast-conserving therapy (BCT) has been offered as the standard care for patients with early breast cancer^[1-3]. Adjuvant radiotherapy (RT), such as whole breast irradiation (WBI) with an additional boost delivered to the lumpectomy cavity (LC) or partial breast irradiation (PBI), is an important component in BCT, as it reduces locoregional recurrence (LRR) and improves overall survival (OS)^[4,5]. Given that adjuvant RT often delivers a therapeutic radiation dose to the clinical target volume and that radiation morbidity is directly related to the irradiated volume, an accurate delineation of the LC is a prerequisite to achieve treatment efficiency and to decrease acute/late toxicity.

To date, as the standard reference imaging modality, computed tomography (CT) simulation imaging has been used to localize the LC^[6,7]. Both titanium surgical clips and seromas are important markers for delineating the LC based on CT simulation images^[8,9]. Many previous studies have advocated that various landmarks, such as the number and location of titanium surgical clips and the seroma clarity score (SCS)^[10], within the excision cavity can influence the accuracy of LC delineation^[7,8,12]. According to previous studies, interobserver variation decreases significantly as the SCS increases, and variability is lowest in patients with an SCS of 3~5^[11,12]. When the SCS is equal to or greater than 3, observer consistency in LC contouring can be improved when the number of surgical clips is 5 to 6^[13]. However, the accuracy of an SCS <3 to mark LCs remains controversial, as seroma visibility is too low for observers to distinguish.

Given the lack of contrast observed on CT images, several investigators have proposed the use of additional image-guided techniques. On account of the intrinsically high soft tissue contrast of magnetic resonance imaging (MRI), LC can be better identified, hence making it a promising tool in breast RT simulation^[14]. When seroma is visible, noncontrast MRI also improves the LC SCS, interobserver concordance and accuracy for patients without clips in the LC compared to CT simulation imaging^[15-17]. If the SCS is too low to be determined, it seems that no valid information can be obtained, even from CT and noncontrast MR coregistered images^[18,19].

Several studies have shown that LCs can be identified easily on delayed-enhancement MRI (DE-MRI) for patients with with SCS ≥ 3 ^[20,21]. Thus, we compared prone CT simulation images and different sequences of prone DE-MR simulation images for LC delineation in patients whose excision cavity had a low SCS but an appropriate number of titanium surgical clips after breast-conserving surgery (BCS). The better time for acquiring DE-MR simulation images in LC delineation was also analyzed.

Materials And Methods

Patient selection

Patients with early-stage breast cancer (pT1-2; N0; M0) who were treated with BCS were included in our study. The characteristics of the 26 patients studied are listed in Table 1. All patients were suitable for prone RT based on body condition, breast size and LC position. All patients underwent lumpectomy with 5 to 6 titanium surgical clips implanted superior, inferior, medial, lateral, and posterior to the LCs, and when

simulated, the SCS in the surgical cavity was less than or equal to 2. Patients with contraindications for MRI or oncoplastic BCS were excluded, and it was necessary for all patients to cooperate well with breathing training. Written informed consent was obtained from all enrolled patients who voluntarily underwent postoperative DE-MR and CT simulation scans in the prone position. This study was approved by the Institutional Review Board of the Shandong Cancer Hospital and Institute Ethics Committee (SDTHEC201703014).

Image acquisition

Patients underwent postoperative prone CT simulation scans (Philips Medical Systems, Inc., Cleveland, OH) on a patient-specific treatment board (CIVCO Horizon™ Prone Breast Bracket, MTHPBB01) with both arms above the head (Fig. 1). The contralateral breast was abducted adequately, while the treated breast was hung freely away from the chest wall through an opening in the board. As the marks on the ipsilateral breast, back and side were aligned with lasers, noncontrast CT simulation scans were acquired.

Acquired immediately after or on the same day as CT simulation scans, the MR simulation scans were collected with a specially designed 32-element phased-array breast coil by a 3.0-T, 70-cm bore MR scanner (750 W, General Electric Co., Boston, USA). During MR simulation scans, the patients were immobilized with the same dedicated device and in the same position as in CT simulation scans. A total of 4 pulse sequences of MR simulation images were acquired in turn. First, fat-suppressed T2W images with the inhibition of [motion artifacts](#) were acquired with patients under free breathing. This was followed by multiphase delayed-enhancement T1-weighted imaging (DE-T1WI) of the ipsilateral breast with fat suppression, performed at 2 min, 5 min and 10 min postcontrast subtraction with patients under breath holding. The characteristics of all pulse sequences used in this study are summarized in Table 2. All enhanced sequences were injected with 15 mL of contrast agent (gadopentetate dimeglumine) at 2 mL/sec. Afterwards, 20 ml of normal saline was injected to ensure that the contrast agent was fully absorbed into the body.

The slice thickness of both the CT and MR simulation images was 3 mm, and all images were transferred to MIM version 6.8.3 software (Cleveland, USA).

LC delineation

The LCs were manually delineated on CT and MR simulation images by three experienced radiation oncologist. The LCs derived from CT simulation images were based only on the placement of the titanium surgical clips and were defined as LC_{CT} (Fig. 2A1). On T2WI with fat suppression and on DE-T1WI at 2 min, 5 min or 10 min, the LCs were delineated based on the visible MR signal of the surgical cavity and defined as LC_{T2} , LC_{2T1} , LC_{5T1} and LC_{10T1} (Fig. 2A2-5). The LC contours delineated on the fusion of T2WI, 2nd min DE-TIWI, 5th min DE-TIWI and 10th min DE-TIWI to CT simulation images were shown in Fig. 2B2-5. The interval of the delineation of LC_{T2} , LC_{2T1} , LC_{5T1} and LC_{10T1} was 2 weeks. To avoid providing a reference for the new LCs, the LCs that had been contoured were not shown when contouring the new LCs. The time required for LC delineation was also recorded.

Deformable image registration (DIR) procedure

The DIR procedure of CT and MR simulation images consisted of 4 consecutive steps that were implemented using the MIM system. The time taken for DIR was approximately 3 to 5 min per patient. During the DIR procedure in this study, prone CT simulation images represented the main sequence, and prone MR simulation images represented the subordinate sequence. Afterwards, according to the workflow in MIM, the user performed an automatic rigid registration between the CT simulation images and each sequence of the MR simulation images. As rigid registration was approved, DIR was used to resample the MRI data for fusion with the CT data for each patient separately. Finally, based on automatic deformation, the Reg Reveal tool was used for evaluating DIR in the primary area of concern^[22]. Reg Refine would only be used in the event that, while evaluating the initial deformation with Reg Reveal, it was determined a poor alignment was identified that needs to be fixed^[23]. Converting local alignments, defined as an assemblage of local alignments to create a deformable registration, was used in our study. Points of skin, nipple, sternum and ribs were locked by Reg Refine to guarantee better registration of the surgical cavity and treated breast. Then, they were combined into an overall deformable registration after rigid registration was approved. Note that a Gaussian mixing model was used in this combination to spatially weight the contributions of each local rigid alignment. Eventually, the point contours were regarded as a reference by DIR quality assurance (QA) to see how close these markers came to matching after the DIR was ran.

Please see the "Parameter evaluation" section in the supplementary files.

Statistical analysis

The Wilcoxon signed-rank test was used to compare the volume or delineation time of LCs (LC_{CT} versus LC_{T2} , LC_{2T1} , LC_{5T1} or LC_{10T1}) since they did not follow a normal distribution. One-way analysis of variance (ANOVA) was used to compare differences in parameters such as the CI, DI and COM between the CT and MRI cohorts, as was inter(intra)observer variability for LC delineation on different image modalities. The relevance of differences between LC volumes was calculated by Spearman rank correlation analysis. Statistical analysis was performed using SPSS 19.0 software (IBM Corporation, Armonk, NY, USA). A P value < 0.05 was considered significant.

Results

Between September 2018 and July 2019, 26 patients were enrolled in this study, and the median patient age was 45 years (range, 29 to 53 years). Of the 26 patients, 76.92% were diagnosed with ductal carcinoma in situ (DCIS), and the other 23.08% were diagnosed with invasive ductal carcinoma (IDC). All patients underwent a lumpectomy and were confirmed to have negative tumor margins during the single operation. The SCS values on CT simulation images varied from 0 to 2 for the patients studied (median, 0).

The inter(intra) observer variation for LC delineation

The inter- and intraobserver variation (Inter-Clgen and Intra-Clgen) for LC on each image modality are listed in Table 3. The agreement of LC delineation was strongest for 10th min DE-TIWI (COV=2.30%, Inter-Clgen =87.06%, Intra-Clgen =92.64%) followed by T2WI (COV=5.45%, Inter-Clgen =83.69%, Intra-Clgen =92.24%) and the agreement of LC delineation was lowest for CT (COV=8.97%, Inter-Clgen=73.88%, Intra-Clgen=86.83%). The differences among each image modality for Inter-Clgen and Intra-Clgen did not reach statistical significance (all $P > 0.05$).

Comparison of the delineation times

The time required to delineate LC_{T2} , LC_{2T1} , LC_{5T1} and LC_{10T1} accounted for 86.96%, 81.30%, 81.97% and 76.34%, respectively, of that required to delineate LC_{CT} ($P = 0.021, 0.003, 0.001, \text{ and } 0.000$, respectively) (Fig. 3). Furthermore, the time required to contour LC_{CT} and LC_{10T1} showed the largest difference, with a median ratio of 1.31 ($Z = 3.516, P = 0.000$).

Comparison of the LC volumes and correlation analysis

The LC_{CT} , LC_{T2} , LC_{2T1} , LC_{5T1} and LC_{10T1} volumes are listed in Table 4. The LC_{2T1} and LC_{5T1} volumes were 2.20 cm^3 and 1.49 cm^3 larger than the LC_{CT} volume, respectively ($Z = -2.914$ and -2.601 , respectively; $P = 0.004$ and 0.009 , respectively). However, there was no statistically significant difference between the LC_{CT} volume and the LC_{10T1} or LC_{T2} volume ($Z = -1.810$ and -1.855 , respectively; $P = 0.064$ and 0.070 , respectively). The LC_{CT} volume was proven to be significantly positively correlated with those of LC_{T2} , LC_{2T1} , LC_{5T1} and LC_{10T1} ($r = 0.904, 0.852, 0.888, \text{ and } 0.929$, respectively, all $P < 0.05$).

LC comparison

The comparisons of the image registration results are shown in Table 5. When considering the CI, DI and COM, we found that LC_{CT} - LC_{10T1} was better than other sequences, although there were no statistically significant differences between them ($F = 0.580, 0.628$ and 0.935 , respectively; $P = 0.584, 0.661$ and 0.432 , respectively). It was noted that compared to LC_{CT} - LC_{T2} , LC_{CT} - LC_{2T1} and LC_{CT} - LC_{5T1} , the CI and DI were improved by LC_{CT} - LC_{10T1} . They increased by 2.08% and 4.48% for LC_{CT} - LC_{T2} , 11.36% and 2.94% for LC_{CT} - LC_{2T1} , and 8.89% and 7.69% for LC_{CT} - LC_{5T1} , respectively. For all patients in our study, the COM of LC_{CT} - LC_{10T1} decreased by 17.86%, 6.12% and 13.21% compared with that of LC_{CT} - LC_{T2} , LC_{CT} - LC_{2T1} and LC_{CT} - LC_{5T1} , respectively.

Discussion

The current gold standard of LC delineation is using standardized guidelines coupled with CT/seroma and surgical clips when present^[8,24]. However, either seroma or surgical clip has its own limitations in LC contouring, for example, the seroma volume and SCS decrease over time, cases with or without an insufficient number of surgical clips in the excision cavity, and architectural distortion caused by oncological surgical techniques lead to the inconsistency between surgical clips and primary tumor

location [25-31]. Therefore, in our study, all patients were implanted with 5~6 titanium surgical clips in the cavity, as this is considered the optimal number of markers in BCT^[13]. To facilitate the comparison, LC_{CT} delineated based on titanium surgical clips on the CT simulation image was regarded as the reference target in this study.

Until now the advantages of DE-MRI in identifying LC have been shown in several studies^[20,21]. The inter (intra)observer variation for LC delineation on CT and each MRI image modality all showed no significant difference. However, DE-MR and fat-suppressed T2WI yielded better inter(intra)observer variation than CT scans. The concordance of LC delineation was strongest for 10th min DE-T1WI (COV=2.30%, Inter-Clgen =87.06%, Intra-Clgen =92.64%). The Dice coefficient is an effective method to evaluate the performance of the DIR. Previous studies found that the Dice coefficient produced by DIR was 0.65 for CT/MRI and 0.43 for CT/PET-CT^[32,33]. In our study, the Dice coefficient of 0.7 increased by approximately 7.14% or 38.57% compared with other reports. Hence, we explored the best MRI-simulation scanning sequences and the best delayed time further for delineating the LC.

Several imaging modalities, including MRI, ultrasound (US), and positron emission tomography (PET) CT, have been explored to improved the accuracy of LC delineation, but MRI has shown to be superior due to its soft tissue contrast^[14,15,17]. Our results reveal that when patients have an invisible seroma or an inferior SCS, LCs can be distinguished more easily on both fat-suppressed T2WI and fat-suppressed DE-T1WI than on CT simulation images. But noncontrast, nonfat-suppressed MRI does not improve the interobserver concordance of LC delineation compared to CT images even for patients with surgical clips and high SCS^[18,19]. Concerning patients who underwent open cavity surgical techniques with either no surgical clips or poor seroma clarity, Jolicoeur et al. found that interobserver variability generated from T2WI without fat suppression was smaller than that generated from noncontrast CT images for LC delineation^[15]. As shown in Table 3, the inter-Clgen obtained on MR was better than that derived from CT images, implying that the volume and location of the LC achieved better concordance among the three observers based on MR than CT images. This discrepancy may be due to the better LC contrast with normal breast soft tissue of MRI than CT, the various surgical techniques (open- and closed-cavity surgical technique) and so on.

A postoperative complex, which includes seroma contains mixed fat and minimal water signal, and the cavity wall acts as a surrogate for the LC on postoperative MR simulation images^[34]. Previous studies of postoperative MRI have demonstrated correlations between the signal characteristics of nonfat-suppressed T2WI and cavity contents, such as seromas^[15]. However, the cavity wall, formed by granulation tissue, is difficult to detect on nonfat-suppressed T2WI. In a study by DEN et al.^[35], patients with inferior visibility of LC potentially benefited from the use of fat-suppressed T2WI, since there was clear contrast between seroma and fibroglandular tissue. We contoured LC_{T2} (Fig. 2) on fat-suppressed T2WI, as the patients recruited were without a seroma or with a poor SCS (≤ 2). Although no significant difference between the volume of LC_{T2} and that of LC_{CT} was found, the CI and DI between LC_{T2} and LC_{CT} were only 0.48 and 0.67, respectively, indicating that the shapes of the contours being different. When

delineating the LC on fat-suppressed T2WI, close attention should be paid to patients long after surgery who with lower SCS, in which a low cavity wall signal might be the result of the evolution of granulation tissue into fibrous tissue (Fig. 2 A2; SCS=0). However, the time limit remains unclear. The high LC signal remained on fat-suppressed T2WI even though the longest time from surgery in our study was 198 days.

Enhancement can be homogeneous or heterogeneous which may be associated with fat signal intensity, fat necrosis, signal voids, or resolving edema, so breath holding-DE-T1WI acquired by an MR scanner can provide superior soft tissue contrast^[20,36,37]. Hence, we innovatively regard breath holding DE-T1WI as simulation scans for breast cancer patients who underwent prone RT. To explore which DE time points were better in LC delineation for patients with an invisible seroma or a poor SCS, for the first time, we obtained multiphase breath holding-DE-T1WI. It was noted that the enhancement surrounding the DE-T1WI excision cavity progressively increased over time, and LC_{10T1} yielded maximal enhancement. LC_{10T1} was better than other DE time points or T2 in terms of correlations with the LC volume and location. LC_{CT}-LC_{10T1} also offered better spatial overlap than the other DE-T1WI sequences across all patients. LC enhances on contrast MRI is the result of pathophysiological reactions to wound repair, including inflammatory infiltration, granulation tissue proliferation, and the increasing number and permeability of the vasculature. Owing to the structural characteristics of vascularized granulation tissue, contrast material will accumulate at the pericavity during the delayed phase^[14,38]. Among our patients, the median interval after BCS was 122 days, during which the granulation tissue formation might have evolved into fibrous tissue during wound healing. As a result, the granulation tissue where most contrast material flowed in and out (blood clotting, inflammation, and finally tissue remodeling) slowly showed persistent enhancement over time on DE-MRI, and of course, LC_{10T1} had the highest signal around the LC in our study.

Compared with the previous study of LC contouring on MRI, a new scanning sequence (breath holding-DE-MRI) and multiperiod scanning were applied in our study^[18,32]. Though breathing control can decrease respiratory movement-associated artifacts, our results showed that LC_{CT} was smaller than the LC derived from MRI regardless of the scanning sequence used. Breath holding-DE-MRI could provide additional information for LC contouring when compared to CT coupled with surgical clips or dynamic contrast-enhanced T1WI (DCE-T1WI). In addition, we also found that the time required for delineation with DE-MRI was obviously shorter than that with CT, which may be further helpful for radiation oncologists to improve their work efficiency and the accuracy of delineation in the clinic. In the future, we will increase the number of suitable patients to further verify our result, and also further clarify the principle of how delayed time poses an effect on the LC defined by DE-T1WI in our subsequent research.

Conclusions

For patients with a low SCS or an invisible seroma in the surgical cavity after BCS, it is reasonable to use prone DE-T1WI simulation scans to guide LC delineation. The LCs defined at 10 min postinjection with DE-T1W images offered modest coverage compared with the LCs defined with CT simulation images

based on titanium surgical clips regardless of the volumes and locations of the LCs. Inter (intra) variability was minimal for the delineation of the LC based on 10th min DE-TIWI. DIR was used to minimize the spatial dislocation of targets caused by registration between CT and MR simulation images in this work. Prone simulation scans not only aid in LC delineation but also detect LCs located distant from the chest wall, thus avoiding the effect of an enhanced pectoralis on LC delineation.

Declarations

Ethics approval and consent to participate

Approval was obtained from the Institutional Research Ethics Board of the Shandong Tumor Hospital Ethics Committee (SDTHEC201703014).

Consent for publication

All study participants provided informed written consent for publication.

Availability of data and materials

The datasets used and/or analyzed during the current study are available from the corresponding author on reasonable request.

Competing interests

The authors declare that they have no competing interests.

Funding programs

National Natural Science Foundation of China (81703038);

Key Research Development Program of Shandong Province (2017GSF18102);

Key Research Development Program of China (2016YFC090 4700)

Authors' contributions

CHZ contributed to the study design, data statistics and analysis and writing of the manuscript. JBL and WW participated in the study design. GZG made important contributions to CT and MR simulation images. YJZ, FXL, QS, JZW, XJL, MX and LX participated in the implementation of the study.

Acknowledgements

This work was supported by Shandong Cancer Hospital and Institute, China.

Abbreviations

DE-MR delayed-enhancement magnetic resonance

LC lumpectomy cavity

SCS seroma clarity score

BCS breast-conserving surgery

DIR deformable image registration

CT computed tomography

T2WI T2-weighted imaging

DE-T1WI delayed-enhancement T1-weighted imaging

CI conformal index

DI degree of inclusion

COM center of mass

Clgen generalized conformity index

BCT breast-conserving therapy

RT radiotherapy

WBI whole breast irradiation

PBI partial breast irradiation

LRR locoregional recurrence

OS overall survival

MRI magnetic resonance imaging

DE-MRI delayed-enhancement magnetic resonance imaging

3D three-dimensional

LR lateral

AP anteroposterior

SI superoinferior

DCIS ductal carcinoma in situ

IDC invasive ductal carcinoma

DCE-T1WI dynamic contrast-enhanced T1-weighted imaging

References

- [1] Litière S, Werutsky G, Fentiman IS, et al. Breast conserving therapy versus mastectomy for stage I–II breast cancer: 20 year follow-up of the EORTC 10801 phase 3 randomised trial. *Lancet Oncol*. 2012;13(4):412-9.
- [2]. Corradini S, Niyazi M, Niemoeller OM, et al. Adjuvant radiotherapy after breast conserving surgery-A comparative effectiveness research study. *Radiother Oncol*. 2015;114(1):28-34.
- [3]. Fisher B, Anderson S, Bryant J, et al. Twenty-Year Follow-up of a Randomized Trial Comparing Total Mastectomy, Lumpectomy, and Lumpectomy plus Irradiation for the Treatment of Invasive Breast Cancer. *N Engl J Med*. 2002;347(16):1233-1241.
- [4]. Early Breast Cancer Trialists' Collaborative Group (EBCTCG), Darby S, McGale P, et al. Effect of radiotherapy after breast-conserving surgery on 10-year recurrence and 15-year breast cancer death: meta-analysis of individual patient data for 10,801 women in 17 randomised trials. *Lancet*. 2011;378(9804):1707-16.
- [5]. Recht A, Solin LJ. Breast-conserving surgery and radiotherapy in early-stage breast cancer: the importance of local control. *Semin Radiat Oncol* 2011(1); 21: 3–9.
- [6]. Goldberg H, Prosnitz RG, Olson JA, et al. Definition of postlumpectomy tumor bed for radiotherapy boost field planning: CT versus surgical clips. *Int J Radiat Oncol Biol Phys* 2005;63(1):209–13.
- [7]. Kirby AM, Coles CE, Yarnold JR. Target volume definition for external beam partial breast radiotherapy: Clinical, pathological and technical studies informing current approaches. *Radiother Oncol*. 2010, 94 (3): 255-263.
- [8]. Yang TJ, Tao R, Elkhuzen PH, et al. Tumor bed delineation for external beam accelerated partial breast irradiation: A systematic review. *Radiother Oncol*. 2013, 108 (2) :181-9.
- [9]. Weed DW, Yan D, Martinez AA, et al. The validity of surgical clips as a radiographic surrogate for the lumpectomy cavity in image-guided accelerated partial breast irradiation. *Int J Radiat Oncol Biol Phys* 2004;60(2):484–92.
- [10]. Kader HA, Truong PT, Pai R, et al. When is CT-based postoperative seroma most useful to plan partial breast radiotherapy? Evaluation of clinical factors affecting seroma volume and clarity [J]. *Int J Radiat Oncol Biol Phys*. 2008, 72 (4) :1064-9. DOI:10.1016/j.ijrobp.2008.02.049.

- [11].Guo B, Li J, Wang W, et al. Interobserver variability in the delineation of the tumour bed using seroma and surgical clips based on 4DCT scan for external-beam partial breast irradiation. *Radiat Oncol*. 2015;10:66.
- [12].Landis DM, Luo W, Song J, et al. Variability among breast radiation oncologists in the delineation of the postsurgical lumpectomy cavity. *Int J Radiat Oncol Biol Phys*. 2007;67(5):1299-308.
- [13].Wang W, Li J, Xing J, et al. Analysis of the variability among radiation oncologists in delineation of the postsurgical tumor bed based on 4D-CT. *Oncotarget*, 2016,7 (43) :70516-70523.
- [14]. Whipp EC, Halliwell M. Magnetic resonance imaging appearances in the postoperative breast: The clinical target volume tumor and its relationship to the chest wall. *Int J Radiat Oncol Biol Phys*. 2008;72(1):49-57.
- [15]. Jolicoeur M, Racine ML, Trop I, et al. Localization of the surgical bed using supine magnetic resonance and computed tomography scan fusion for planification of breast interstitial brachytherapy. *Radiother Onco*. 100 (2011) 480–484
- [16]. Al-Hammadi N, Caparrotti P, Divakar S, et al. MRI Reduces Variation of Contouring for Boost Clinical Target Volume in Breast Cancer Patients Without Surgical Clips in the Tumour Bed. *Radiol Oncol*. 2017;51(2):160-168.
- [17]. Jacobson G, Zamba G, Betts V, et al. Image-Based Treatment Planning of the Post-Lumpectomy Breast Utilizing CT and 3TMRI. *Int J Breast Cancer*. 2011;2011:246265.
- [18]. Pogson EM, Delaney GP, Ahern V, et al. Comparison of Magnetic Resonance Imaging and Computed Tomography for Breast Target Volume Delineation in Prone and Supine Positions. *Int J Radiat Oncol Biol Phys*. 2016;96(4):905-912.
- [19]. Mast M, Coerkamp E, Heijenbrok M, et al. Target volume delineation in breast conserving radiotherapy: are co-registered CT and MR images of added value? *Radiat Oncol*. 2014;9:65.
- [20]. Drukteinis JS, Gombos EC, Raza S, et al. MR imaging assessment of the breast after breast conservation therapy: distinguishing benign from malignant lesions. *Radiographics*. 2012;32(1):219-34.
- [21]. Mahoney MC, Sharda RG. Postoperative enhancement on breast MRI: Time course and pattern of changes. *Breast J*, 2018, 24(5):783-788.
- [22].Pirozzi S , Piper J , Nelson A , et al. A Novel Framework for Deformable Registration Evaluation and Quality Assurance. *Int J Radiat Oncol Biol Phys*, 2013, 87(2):S719.
- [23].Pirozzi S , Piper J , Nelson A , et al. A Novel Framework for User-Intervened Correction of Deformable Registration. *Int J Radiat Oncol Biol Phys*, 2013, 87(2):S144.

- [24]. <http://www.rtog.org/LinkClick.aspx?fileticket=vzJFPaBipE%3d&tabid=236>.
- [25]. Moon SH, Shin KH, Kim TH, et al. Dosimetric comparison of four different external beam partial breast irradiation techniques: three-dimensional conformal radiotherapy, intensity-modulated radiotherapy, helical tomotherapy, and proton beam therapy. *Radiother Oncol*. 2009;90(1):66-73.
- [26]. Dzhugashvili M, Tournay E, Pichenot C, et al. 3D-conformal Accelerated Partial Breast Irradiation treatment planning: the value of surgical clips in the delineation of the lumpectomy cavity. *Radiat Oncol*. 2009;4:70.
- [27]. Landis DM, Luo W, Song J, et al. Variability among breast radiation oncologists in delineation of the postsurgical lumpectomy cavity. *Int J Radiat Oncol Biol Phys*. 2007;67(5):1299-308.
- [28]. Yang Z, Chen J, Hu W, et al. Planning the breast boost: how accurately do surgical clips represent the CT seroma? *Radiother Oncol*. 2010;97(3):530-4.
- [29]. den Hartogh MD, van den Bongard HJ, Davidson MT, et al. Full-thickness closure in breast-conserving surgery: the impact on radiotherapy target definition for boost and partial breast irradiation. A multimodality image evaluation. *Ann Surg Oncol*. 2014;21(12):3774–9.
- [30]. Madeley CR, Kessell MA, Madeley CJ, et al. Radiographer technique: Does it contribute to the question of clip migration. *J Med Imaging Radiat Oncol*. 2015;59 (5):564-70.
- [31]. Schaverien MV, Stallard S, Dodwell D, et al. Use of boost radiotherapy in oncoplastic breast-conserving surgery - a systematic review. *Eur J Surg Oncol*. 2013;39 (11) :1179-85.
- [32]. Huang W, Currey A, Chen X, et al. A comparison of lumpectomy cavity delineations between use of magnetic resonance imaging and computed tomography acquired with patient in prone position for radiation therapy planning of breast cancer. *Int J Radiat Oncol Biol Phys*. 2016;94(4):832-840.
- [33]. Lee YS, Kim KJ, Ahn SD, et al. The application of PET-CT to post-mastectomy regional radiation therapy using a deformable image registration. *Radiat Oncol*. 2013;8:104.
- [34]. Li J, Dershaw DD, Lee CH, et al. Breast MRI after conservation therapy: usual findings in routine follow-up examinations. *AJR Am J Roentgenol*. 2010, 195(3):799-807
- [35]. DEN Hartogh MD, Philippens ME, VAN Dam IE, et al. Post-lumpectomy CT-guided tumor bed delineation for breast boost and partial breast irradiation: Can additional pre- and postoperative imaging reduce interobserver variability?. *Oncol Lett*. 2015;10(5):2795-2801.
- [36]. EL-Adalany MA, Hamed EED. Role of dynamic contrast enhanced MRI in evaluation of post-operative breast lesions. *The Egyptian Journal of Radiology and Nuclear Medicine*, 2016, 47: 631–640.

[37]. Muir T, Ebrahim L, Wylie E, Taylor D. Review and audit of the post-surgical MRI breast: Pictorial essay. *J Med Imaging Radiat Oncol.* 2019;63(2):163-169.

[38]. Ford EC, Lavelly WC, Frassica DA, et al. Comparison of FDG-PET/CT and CT for delineation of lumpectomy cavity for partial breast irradiation. *Int J Radiat Oncol Biol Phys.* 2008;71(2):595-602.

Tables

Table 1 Characteristics of 26 patients studied

Characteristics	No. of cases (%)
Age (y), median (range)	45 (29-53)
Breast side	
Left	12 (46.15)
Right	14 (53.85)
Tumor Location	
OUQ	12 (46.15)
OLQ	2 (7.69)
IUQ	7 (26.92)
ILQ	0 (0.00)
Central portion of breast	5 (19.23)
Stage	
T1b	7 (26.92)
T1c	16 (61.54)
T2	3 (11.54)
Pathologic type	
IDC	20 (76.92)
DCIS	6 (23.08)
SCS	
0	16(61.54)
1	7(26.92)
2	3(11.54)
No. of titanium surgical clips	
5	17(65.38)
6	9(34.62)
Time interval from surgery to planning CT scan (days), median (range)	122 (30-198)

Abbreviations: *OUQ* = outer upper quadrant; *OLQ* = outer lower quadrant; *IUQ* = inter upper quadrant; *ILQ* = inter lower quadrant; *DCIS* = Ductal carcinoma in situ; *IDC* = Invasive ductal carcinoma; *SCS* = seroma clarity score

Table 2 Parameters of MR simulation pulse sequences

	T2WI	2nd min DE-TIWI	5th min DE-TIWI	10th min DE-TIWI
TR/TE (ms)	7059/81	4.7/2	4.7/2	4.7/2
Slice thickness (mm)	3	3	3	3
FOV (mm)	420	420	420	420
Acquisition time(sec.)	450	18	18	18
Acquisition matrix	256×292	256×292	256×292	256×292

Abbreviations: *TR* = Time of repeatation; *TE* = Time of echo; *FOV* = Field of view

Table 3 Inter- and intra-observer COV and CIgen for LC volumes (% , Mean)

Image modality	COV	Inter-CIgen	Intra-CIgen
CT	8.97	73.88	86.83
T2WI	5.45	83.69	92.24
2nd min DE-TIWI	8.20	82.52	91.22
5th min DE-TIWI	8.48	81.91	90.21
10th min DE-TIWI	2.30	87.06	92.64

Abbreviations: *COV*= coefficient of variation; *CIgen* = generalized conformity index

Table 4 LC volumes delineated based on prone CT simulation images and different prone MR simulation images (cm³)

LC volume	Median (cm ³)	Range (cm ³)	Z-value	P-value
LC _{CT}	9.96	6.44~17.09		
LC _{T2}	12.28	7.26~17.59	-1.855	0.064
LC _{2T1}	12.16	8.41~20.80	-2.914	0.004
LC _{5T1}	11.45	8.23~19.56	-2.601	0.009
LC _{10T1}	14.62	7.30~20.64	-1.810	0.070

Abbreviations: *LC_{CT}*= the LC delineated based on CT simulation images; *LC_{T2}*= the LC delineated based on T2WI; *LC_{2T1}*= the LC delineated based on 2nd min DE-TIWI; *LC_{5T1}*= the LC delineated based on 5th min DE-TIWI; *LC_{10T1}*= the LC delineated based on 10th min DE-TIWI

Table 5 Parameter evaluation of the LC defined using prone CT simulation images and different prone MR simulation images based on DIR

	$LC_{CT}-LC_{T2}$		$LC_{CT}-LC_{2T1}$		$LC_{CT}-LC_{5T1}$		$LC_{CT}-LC_{10T1}$		<i>F</i> -value	<i>P</i> -value
	Median	Range	Median	Range	Median	Range	Median	Range		
CI	0.48	0.35~0.56	0.44	0.39~0.58	0.45	0.30~0.55	0.49	0.38~0.56	0.584	0.628
DI	0.67	0.57~0.75	0.68	0.60~0.84	0.65	0.56~0.79	0.7	0.56~0.85	0.661	0.58
COM(cm)	0.56	0.40~0.73	0.49	0.38~0.70	0.53	0.37~0.70	0.46	0.31~0.80	0.935	0.432

Abbreviations: *CI* = Conformal index; *DI* = Degree of inclusion; *COM* = the distance between the center of mass of the targets; LC_{CT} = the LC delineated based on CT simulation images; LC_{T2} = the LC delineated based on T2WI; LC_{2T1} = the LC delineated based on 2nd min DE-TIWI; LC_{5T1} = the LC delineated based on 5th min DE-TIWI; LC_{10T1} = the LC delineated based on 10th min DE-TIWI

Figures

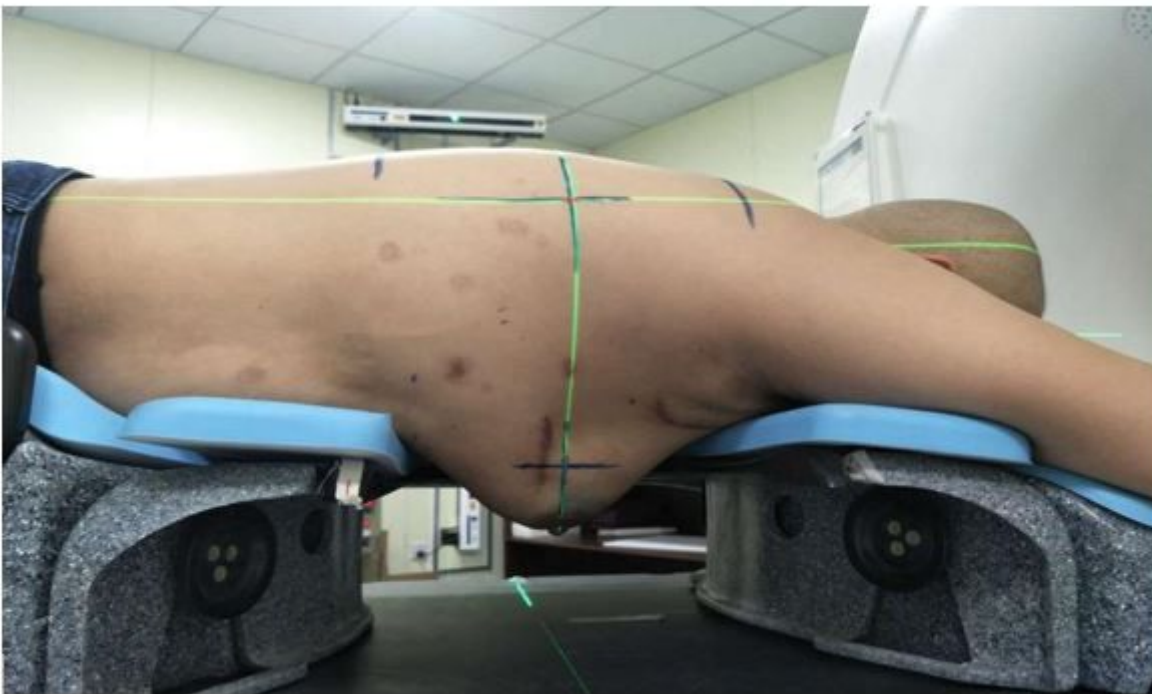


Figure 1

Prone treatment board and placement of markers before simulation scanning

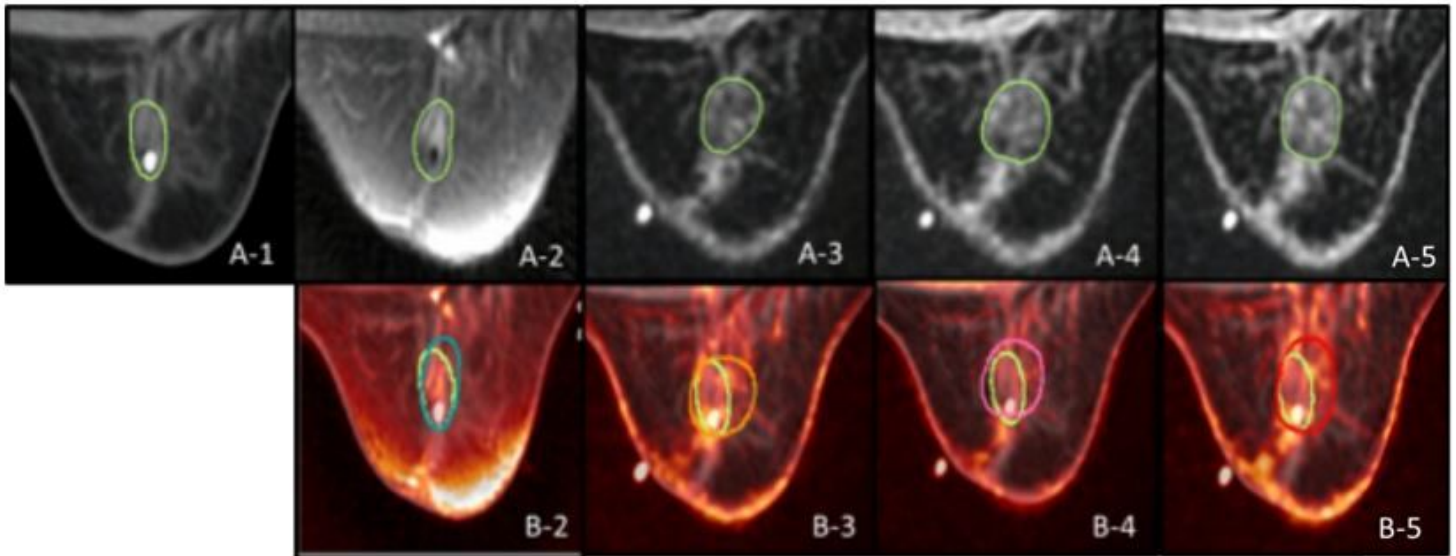


Figure 2

Contours of LC and the comparison of LC on fusion images between different sequences of MRI and CT scans (A-1: LC contours delineated on CT simulation axial images based on titanium surgical clips ; A-2~5:LC contours delineated on T2WI, 2nd min DE-TIWI, 5th min DE-TIWI and 10th min DE-TIWI based on the signal of cavity boundaries. B-2~5: LC contours delineated on the fusion of T2WI, 2nd min DE-TIWI, 5th min DE-TIWI and 10th min DE-TIWI to CT simulation axial images, respectively)

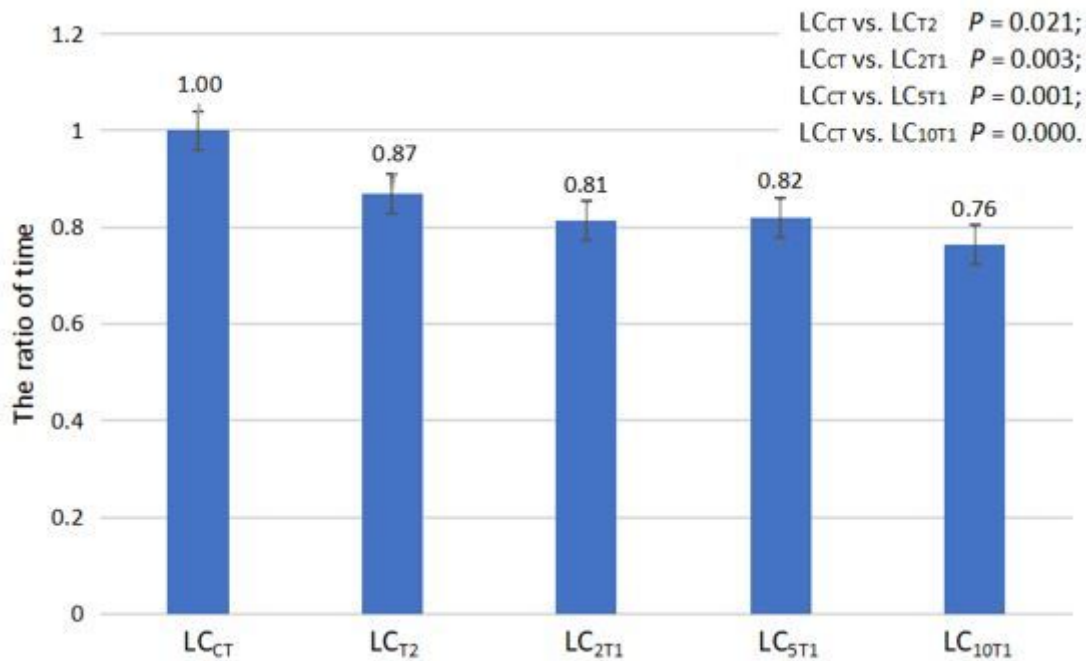


Figure 3

The ratio of time required to delineate the LCs based on prone CT simulation images and various sequences of prone MR simulation images

Supplementary Files

This is a list of supplementary files associated with this preprint. Click to download.

- [ROMRIcoverletter.docx](#)
- [renamed61710.pdf](#)